

## Effect of Front Wall Geometry and Orifice Shape of Oscillating Water Column Device: Numerical investigation

Ayaz Al Abrar, Abdullah Al-Faruk\*, Muhammad Sazid Shahriar

Department of Mechanical Engineering, Khulna University of Engineering & Technology, Khulna-9203, Bangladesh

### ABSTRACT

This research investigates the performance of oscillating water column (OWC) devices in wave energy conversion system, emphasizing the influence of front wall geometry and orifice shape. As OWC systems are promising renewable energy technologies, optimizing their design can lead to significant gains in efficiency. This study uses computational fluid dynamics (CFD) simulations to systematically explore various configurations of front wall shapes and orifice geometries, aiming to understand their effects on the air-water interactions within the OWC chamber. The core objectives include analyzing pressure distributions, examining flow dynamics, and evaluating energy conversion efficiency across multiple design parameters and operational conditions. The numerical simulations yield valuable insights into OWC performance. Results show that a rounded front wall lip enhances efficiency by 15.3% compared to conventional designs, while a triangular lip shape results in a 10.1% decrease in performance. In terms of orifice configurations, the converging orifice demonstrates a 1.9% efficiency improvement over the standard shape, whereas a diverging orifice reduces efficiency dramatically by 60.36%. These findings highlight the critical impact of structural design on the effectiveness of OWC devices in converting wave energy into usable power. Employing advanced CFD techniques and validating results with experimental data, this study provides practical recommendations for optimizing OWC systems. By illuminating the nuanced relationships between front wall and orifice designs and their performance outcomes, the research contributes to an improved understanding of OWC dynamics. The results underscore the importance of geometry and design choices in OWC technology, offering meaningful insights that can guide the development of more efficient and sustainable wave energy solutions. Ultimately, this study supports the advancement of renewable energy systems as a pathway to a cleaner, sustainable energy future.

Keywords: Wave Energy Converter, Oscillating Water Column Device, Numerical Wave Tank, Front Wall Geometry



Copyright @ All authors

This work is licensed under a [Creative Commons Attribution 4.0 International License](https://creativecommons.org/licenses/by/4.0/).

### 1. Introduction

The global energy landscape has been significantly influenced by pivotal events such as the 1973 oil crisis, prompting a concerted effort to explore renewable energy technologies due to concerns over rising fossil fuel costs and environmental degradation [1]. Alongside solar, hydro, tidal, geothermal, and biomass sources, wave energy has emerged as a promising avenue for sustainable energy generation [2]. Noteworthy for its high energy density, minimal environmental impact, and predictable nature, wave power offers a reliable renewable energy alternative [3]. In response to varying energy-absorbing processes and device locations, numerous wave energy conversion models have been proposed [4].

Central to this endeavor is the oscillating water column (OWC) device, which has garnered attention for its simplicity and effectiveness in converting wave energy into usable power [5]. Comprising a partially submerged chamber open below the water's surface, the OWC device captures wave energy by oscillating air within the chamber, driving an electricity-generating turbine [6]. Unlike some wave energy converters (WECs), OWCs boast simplicity with no underwater moving parts, resulting in user-friendly operation and minimal maintenance requirements [7]. They offer versatility in application, integrating seamlessly into various coastal structures or deployed independently [8].

While OWC systems near shorelines have received considerable attention for their direct wave energy capture, research into their efficacy in open ocean environments remains limited [9]. Challenges arise in optimizing energy absorption from incident waves in open seas, where wave interactions with the structure are less direct [10]. Balancing energy capture efficiency with structural durability poses a conundrum for OWC deployment in offshore settings, underscoring the need for comprehensive investigation [11]. Vortex shedding at the OWC chamber's sharp edge enhances spatial non-uniformity, impacting device efficiency [12]. An intermediate PTO damping can optimize energy absorption, with wave height affecting device performance differently based on wave periods [13]. The hybrid system is found to improve efficiency over a broader range of wave conditions, making it a promising solution for seaport breakwaters [14]. The integration with a horizontal plate enhances device performance, and a smaller immersed depth is advantageous for energy extraction. Comparisons with breakwater-integrated OWC highlight the plate-integrated system's potential for wave energy utilization [15]. Optimization of dimensions, materials, and structural integrity, highlighting the efficacy of specific design parameters have a significant effect on wave generation and structural stability [16]. The effect of wave steepness on ocean waves in intermediate depths, demonstrating good agreement between numerical and analytical results and emphasizing the importance of

accurately modeling wave behavior for coastal engineering applications [17]. Certain wall angles significantly impact power output and efficiency, offering insights into maximizing energy conversion from progressive waves [18].

A study on the effects of front lip submergence on pressure and velocity in an OWC device designed to use in a coastal region of Bangladesh concluded that that as minimum as possible lip submergence yields the highest pressure in the chamber and velocity through the orifice, enhancing energy output [19]. A two-phase CFD modelling that investigates the chamber geometry of OWC device concluded that smaller orifice diameters improve velocity, pressure, and power output but reduces the efficiency, while rectangular chambers achieve higher instantaneous power than trapezoidal chambers [20].

In light of the above literature survey, it is evident that the front wall geometry of the OWC chamber and the orifice shape is not investigated yet. To better understand how various geometrical parameters might impact the performance of OWC devices, this research project uses CFD to model the efficiency of OWC devices. The researchers want to show the potential advantages of using CFD for this kind of problem and how it can help in optimizing the design of OWC devices by contrasting the numerical results with actual data. The study will entail adjusting various parameters, such as the chamber's shape and location of the opening, and evaluating how they affect the device's ability to capture energy. The current study investigated four cases of front wall lip shape and three cases of orifice shape; namely solenoidal, diverging and converging are investigated through a two-phase computational modeling.

## 2. Numerical methodology

This study intends to assess the effectiveness of an oscillating water column (OWC) device by using computational fluid dynamics (CFD). The purpose is to evaluate the possibility of CFD as an alternative to physical experimentation and to acquire a greater understanding of the characteristics that may affect OWC efficiency. Although physical experimentation is frequently regarded as a trustworthy way to get data on hydrodynamic flow, it can be time-consuming, expensive, and labor-intensive. OWC efficiency may be modeled numerically, however due to simplifications made or the inability to take into account particular geometric aspects, these approaches may produce erroneous findings.

The research will proceed in several stages. The first stage is the development of a 2-D numerical wave tank using CFD. The extension of the numerical wave tank to include a detailed OWC model is in the second stage. Third stage is evaluating the impact of various OWC geometrical parameters on effectiveness. Matching the numerical results for comparison and validation with the data from the real world is in the fourth stage. Finally, the benefits of optimization may have on the design of the OWC device and the effects that site characteristics have on the performance of the device is prediction in the real world.

### 2.1 CFD analysis

The differential form of the laws of mass, momentum, and energy conservation is represented by the continuity equation, Navier-Stokes equations, and energy equation, respectively, are solved using the computer as part of the computational fluid dynamics (CFD) modeling process. To

enable numerical computation within the given domain, these partial differential equations are then approximated as finite-volume expressions and reformed into algebraic equations that are solved in the ANSYS-Fluent software. Fluent has several multi-phase flow features that are relevant to the current case of study. The VOF method is used to track the air-water interface inside the domain. This is crucial for the accurate modeling of the hydro-pneumatic interaction within the OWC chamber, in addition to being important as a way to delineate the interface. To allow for finite analytical times or to explain phenomena that are not yet fully understood, simplifications and approximations must be made, as is the case with any numerical modeling (e.g., turbulence). To incorporate real-world conditions that were not anticipated during the development of the numerical model, the chosen modeling tool may need to be validated experimentally. Studies are carried out to assess these effects for specific geometric arrangements.

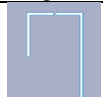

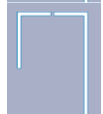

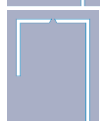
### 2.2 Pre-processing

As a critical step in the pre-processing phase of CFD simulations, the geometry of the system must be carefully defined. This involves selecting an appropriate device size and surrounding computational domain to ensure realistic outcomes while minimizing boundary-induced effects, such as wave reflections. The model configuration also includes generating a computational mesh to discretize the domain into smaller control volumes. The boundary conditions, the wave generation mechanism, must be meticulously specified to replicate real-world conditions with accuracy.

The geometrical model of a wave tank simulation should be carefully designed to ensure that the results are accurate and representative of the real system. This includes selecting the appropriate size and shape of the tank, wave generator, and model, and applying the correct boundary conditions.

The geometrical model of the computational fluid domain is developed using a DesignModeler in ANSYS-Fluent. First a rectangular channel  $34 \times 10$  m has been drawn. Then column is drawn which has dimension of 7 m length, orifice diameter 0.2 m and thickness 0.25 m have been taken. The description of study cases and the corresponding geometry is given in Table 1.

**Table 1** Different cases of OWC devices.

| Description  | Figure  |
|--|---|
| <b>Case 1:</b> Geometry of a base OWC device   |  |
| <b>Case 2:</b> Geometry of a rounded lip frontal wall. The frontal wall has a circular shape of 0.25 m diameter.       |  |
| <b>Case 3:</b> Geometry of a triangular lip frontal wall. The frontal wall has a triangular end which has a 90° angle. |  |
| <b>Case 4:</b> Geometry of a diverging orifice. A 60° angle is present between two adjacent walls.                     |  |
| <b>Case 5:</b> Geometry of a converging orifice. A 60° angle is present between two adjacent walls.                    |  |

2.3 Numerical set-up

The evaluation of wave profiles and the efficiency of OWC devices involves monitoring several parameters; however, numerous additional variables, datasets, and graphical outputs can be obtained both during the simulation and post-processing stages. Free surface elevations at specific time instances are determined using the software's built-in functions, which generate contours for defined quantities. To obtain free surface plots, data corresponding to a Volume of Fluid (VOF) fraction of 0.5 is extracted, as this value identifies the interface between the air phase (VOF=0) and the water phase (VOF=1) within each interface cell. Velocity distributions within the domain can be obtained by defining a 'line' along which flow properties are extracted at specific time steps as shown in Fig.1. Both the free surface elevations and velocity profiles are essential for conducting validation exercises.

The numerical results of a wave tank simulation refer to the outcome of the simulation in terms of quantifiable data, such as wave height, wave period, wave direction, and fluid velocity. These results provide insight into the behavior of the fluid system under different wave conditions and are an important tool for evaluating the performance of the system.

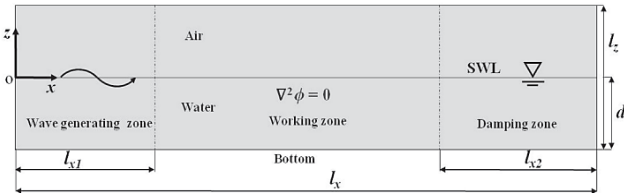


Fig.1 Wave generation in a wave tank.

2.4 Meshing and boundary conditions

The mesh of a wave tank simulation is an important aspect of the simulation as it affects the accuracy and computational efficiency of the simulation. The mesh of a wave tank simulation should be carefully designed to ensure that the results are accurate and representative of the real system. This includes selecting the appropriate grid size, grid quality, grid resolution, and grid refinement. The mesh of the computation domain can be seen in Fig.2. A mesh sensitivity analysis is carried out to confirm independency of mesh in the numerical results. The number of elements and nodes after the sensitivity analysis for different cases of the study is shown in Table 2.

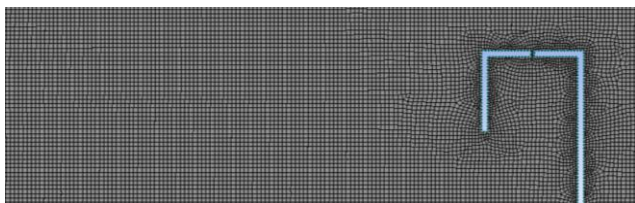


Fig.2 Generated mesh of the wave tank.

It is necessary to specify the information on the flow variables at the domain boundaries. The moving wall at the left of the computation domain is controlled by a User Defined Function (UDF) code. The boundary conditions and the two phases can be seen in Fig.1.

Table 2 No of nodes and elements for different cases.

| Case no. | Name               | No. of elements | No. of nodes |
|----------|--------------------|-----------------|--------------|
| 1        | Base               | 9361            | 9731         |
| 2        | Rounded Lip        | 9442            | 9813         |
| 3        | Triangular Lip     | 9386            | 9754         |
| 4        | Diverging Orifice  | 9369            | 9736         |
| 5        | Converging Orifice | 9354            | 9720         |

Table 3 Material Properties.

| Material | Phase type | $\rho$ (kgm <sup>-3</sup> ) | $\mu$ (N.sm <sup>-2</sup> ) | T (°C) |
|----------|------------|-----------------------------|-----------------------------|--------|
| Air      | Primary    | 1.225                       | 1.7894×10 <sup>-5</sup>     | 20     |
| Water    | Secondary  | 1000                        | 1.003×10 <sup>-3</sup>      | 20     |

2.5 Wave Properties

Wave properties are generated by using wave make theory and the wave equations. Table 3 showing the fluid properties for both the air and water phases in the computational domain. The wave parameters are shown in Fig.3 and the properties of the wave are given in Table 3.

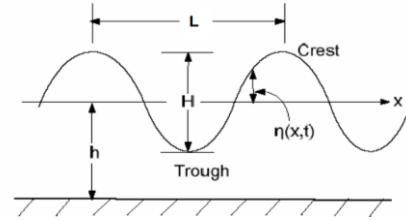


Fig.3 Basic parameters of a sinusoidal waves.

Table 4 The general wave properties.

| Properties                  | Symbol               | Value | Unit               |
|-----------------------------|----------------------|-------|--------------------|
| Wave length                 | <i>L</i>             | 28.24 | m                  |
| Time Period                 | <i>T</i>             | 4     | s                  |
| Wave Depth                  | <i>h</i>             | 5     | m                  |
| Wave Number                 | <i>k</i>             | 0.22  | m <sup>-1</sup>    |
| Celerity                    | <i>c<sub>g</sub></i> | 5.25  | ms <sup>-1</sup>   |
| Water Density               | $\rho$               | 1000  | Kg.m <sup>-3</sup> |
| Acceleration due to gravity | <i>g</i>             | 9.81  | ms <sup>-2</sup>   |
| Wave Height                 | <i>H</i>             | 1.56  | m                  |
| Device Width                | <i>b</i>             | 0.56  | m                  |

In this method, the wave height is calculated from the simulation data by subtracting the maximum and minimum water depth at a certain position during the flow. And the value is 1.56 m. The wave height can also be calculated by the wave maker theory equation shown below:

$$H = \frac{2(\cosh 2kh - 1)}{\sinh 2kh + kh} \times S = 1.73 \text{ m} \quad (1)$$

There is a slight deviation in the wave height values as the theoretical value is a little higher than the analyzed value.

2.6 Wave Parameters

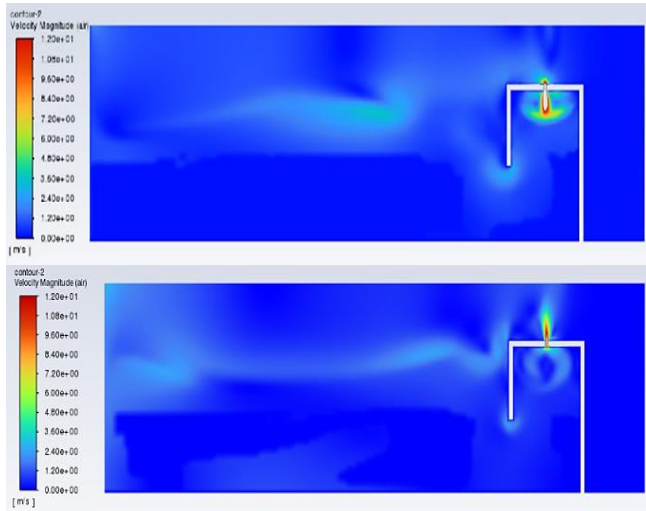
The wave parameters are set on the basis of wave maker theory where different wave heights are calculated for different stroke lengths of the moving wall. The stroke length, wave height and length are shown in Table 5. Three types of waves are analyzed and according to that the 2 phase VOF model is developed.

**Table 5** Wave parameters.

| Types | Stroke Length,<br><i>S</i> (m) | Wave Height,<br><i>H</i> (m) | Wave Length<br><i>L</i> (m) |
|-------|--------------------------------|------------------------------|-----------------------------|
| 1     | 1.2                            | 1.29                         | 27.82                       |
| 2     | 1.6                            | 1.56                         | 28.28                       |
| 3     | 2                              | 1.83                         | 28.74                       |

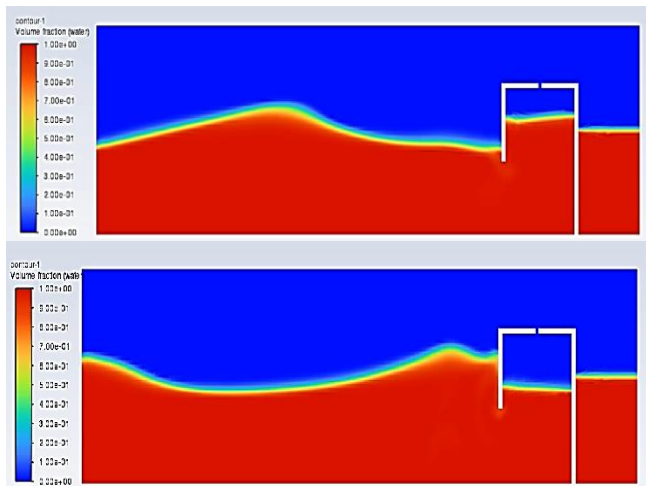
**3. Results and discussions**

A series of simulations are carried out using the two-phase VOF based numerical model to investigate the effects of front wall shape and the orifice shape. The numerical model is validated against the experimental results in terms of pressure and velocity in orifice of the OWC chamber. It is found that the numerical results strongly agree with the published results and the error is minor.



**Fig.4** Contour of fluid velocity during suction (up) and compression (below).

The velocity contours across the two phases are shown in Fig.4 for both the suction and compression strokes. At an arbitrary flow time, the velocity is seen maximum at the orifice zone than others zone. Because air always flows from high pressure zone to low pressure through orifice by converting pressure energy into kinetic energy.

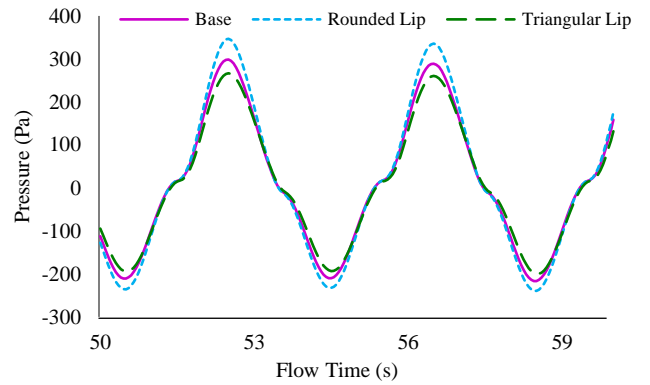


**Fig.5** Contour of phases when OWC chamber is in compression (up) and suction (down).

The water and air phases are presented in Fig.5 during the trough and the crest just before the OWC chamber. At a time, summation of the volume fraction of air (primary phase) and water (secondary phase) is one. The relative motion of air-water inside the computational domain creates numerical wave is seen.

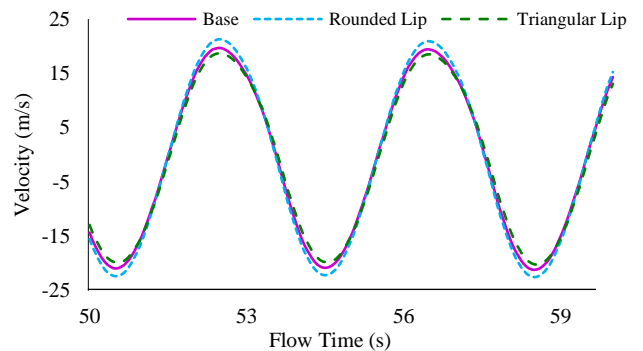
**3.1 Effect of frontal wall geometry**

For a given incident wave, the output pressure at the orifice is greater in rounded lip and less in triangular lip than that of the base. It can be seen in Fig.6 that in terms of pressure, rounded lip has superiority than other two cases. The rounded lip has peak pressure of 346 Pa, whereas base case has 289 Pa and triangular lip has 260 Pa. If pressure at opposite direction is taken into consideration rounded lip has peak pressure of 236 Pa, but base case and triangular lip has peak pressure of only 210 Pa and 193 Pa, respectively.



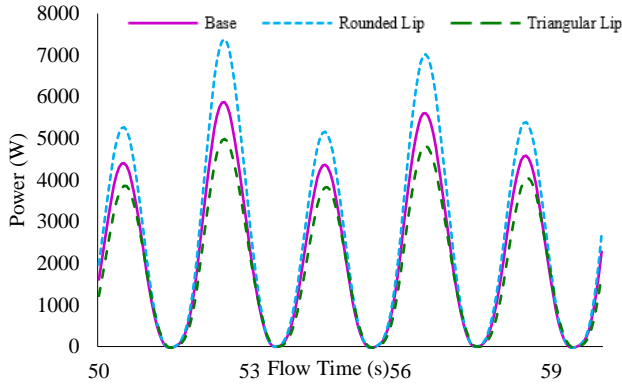
**Fig.6** Time history of pressure for different frontal lips.

The output velocity in the upward direction of the orifice is greater in rounded lip and less in triangular lip than that of the base for a given incident wave. Just like pressure, rounded lip shows slightly better results than the base case as manifested in Fig.7. It has peak velocity of 21 m/s and 22 m/s at opposite directions. But base case has peak velocity of 18.5 m/s and 20 in opposite direction. The triangular lip has 18.26 m/s and 19 m/s peak velocities in two directions.



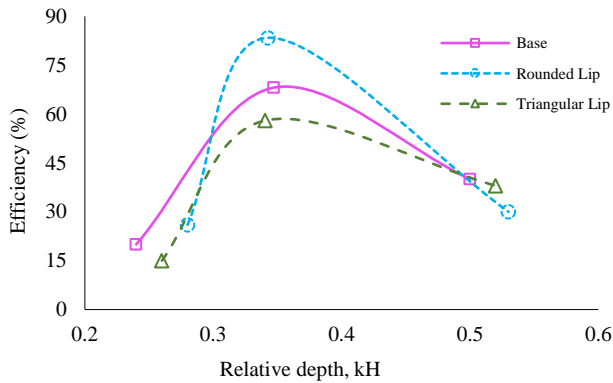
**Fig.7** Time history of velocity for different frontal lips.

The output power of OWC is calculated for the same three cases and undoubtedly the rounded lip is maximum among the cases as evident in Fig.8. This is because of the energy loss due turbulence and flow separation is low for more smoother rounded lip case than the other two. It has peak power of over 7 kW, on the other hand base case and triangular lip has nearly 6 kW and below 5 kW, respectively.



**Fig.8** Time history of power for different frontal walls.

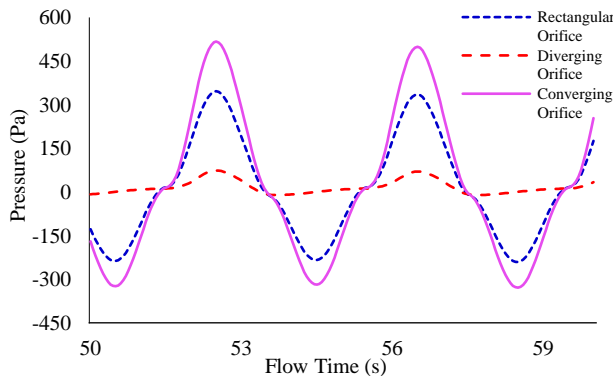
The efficiency is observed with respect to the relative depth,  $kH$ ; dimensionless parameter to compare the maximum value among them. From the plot presented in Fig.9, it is seen that the maximum efficiency can be obtained from rounded lip setup of OWC frontal wall. It has maximum efficiency of 83.4%, which is higher value than the base case and triangular lip that have maximum efficiency of 68.1% and 58%, respectively. Hence, it is undoubtedly evident that the rounded lip is more efficient capturing the wave energy than the other two frontal wall shapes taken into analysis.



**Fig.9** Efficiency of the wave tank for different front walls.

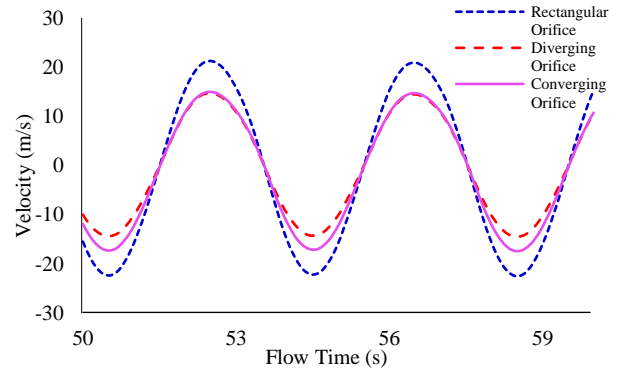
### 3.2 Effect of orifice shapes

Based on the above analysis it is seen that rounded lip has maximum efficiency than other cases. Therefore, to analyze the orifice shape, different orifice shapes are taken into consideration for a single rounded lip shape so that an optimum efficiency can be obtained.



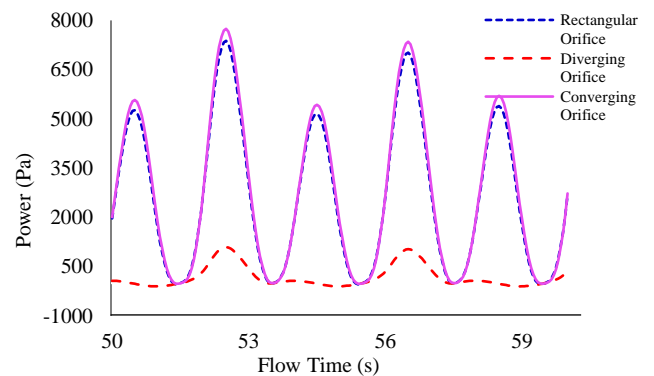
**Fig.10** Time history of pressure for different orifice shapes.

For a given incident wave, the output pressure at the orifice is greater in converging orifice and less in diverging orifice than that of the rectangular orifice. It is seen in Fig.10 that, converging orifice has superiority than other two cases in terms of OWC chamber pressure. The converging orifice has peak pressure of 517.6 Pa, whereas the rectangular orifice has 345 Pa and diverging orifice has only 73.86 Pa. If pressure at opposite direction is taken into consideration converging orifice has peak pressure of 317.14 Pa, but the rectangular orifice has 232.58 Pa and the diverging orifice has no pressure in the opposite direction.



**Fig.11** Time history of velocity for different orifice shapes.

For a given incident wave, the output velocity in the upward direction of the orifice is greater in rectangular orifice and less in diverging and converging orifice similar to pressure variation. Unlike the previous property converging orifice has less velocity than the rectangular orifice as in Fig.11. It has peak velocity of 15 m/s and 17.1 m/s at opposite directions. But the rectangular orifice has peak velocity of 20.66 m/s and 22.11 m/s in opposite direction. Finally, the diverging orifice has 15 m/s and 14.21 m/s peak velocities in the upward and downward directions.

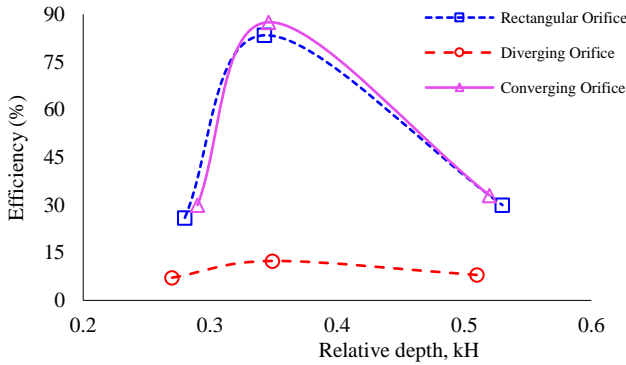


**Fig.12** Time history of power for different orifice shapes.

Finally, the output power of the OWC device is calculated for the same cases of orifice shape. It is clearly seen in Fig.12 that the output power of converging orifice is maximum among the cases. It has peak power of nearly 7750 W, on the other hand the rectangular orifice has slightly low power output of 7450 W. Lastly, diverging orifice has nearly 1000 W of power which is least of them.

The efficiency of OWC device is observed with respect to relative depth,  $kH$ ; a dimensionless parameter to compare the maximum value among them. From the Fig.13, it is seen that the maximum efficiency can be obtained from

converging lip setup. It has maximum efficiency of 87.5%, which is higher value than the rectangular orifice and diverging orifice that have maximum efficiency of 83.4% and 12.4% respectively. Hence, it is very much clear that converging orifice with rounded lip is more efficient than all other cases taken into analysis.

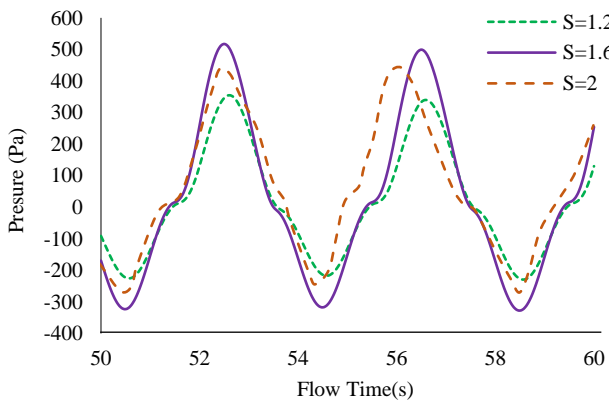


**Fig.13** Efficiency of the wave tank for different orifice shapes.

### 3.3 Effect of stroke lengths

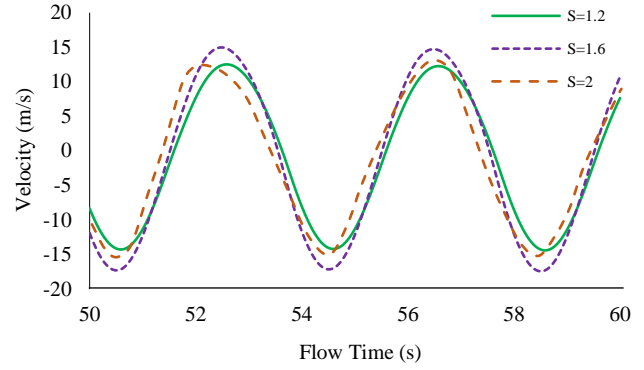
Based on analysis of frontal wall shape and orifice shape analysis, it is seen that rounded lip with converging orifice has maximum efficiency than all other cases. Hence, to analyze the effect of wave properties, different stroke lengths are taken into consideration for a single rounded lip with converging orifice shape so that maximum efficiency can occur in the current study setup. The wave heights are calculated with respect to different stroke lengths according to Table 5. The considered stroke lengths are  $S = 1.2$ ,  $S = 1.6$  and  $S = 2$ .

For a given incident wave, the output pressure at the orifice is maximum for  $S = 1.6$ . Next, it is the 2 m stroke length where the second-best pressure output occurs. And then it comes for the stroke length of 1.2 m. For  $S = 1.6$ , the maximum pressure in one direction is 517.16 Pa, for  $S = 2$  it becomes 438.58 Pa and for  $S = 1.2$ , it becomes 346.93 Pa. So, for a specific range of stroke lengths the pressure output becomes maximum as shown in Fig.14.



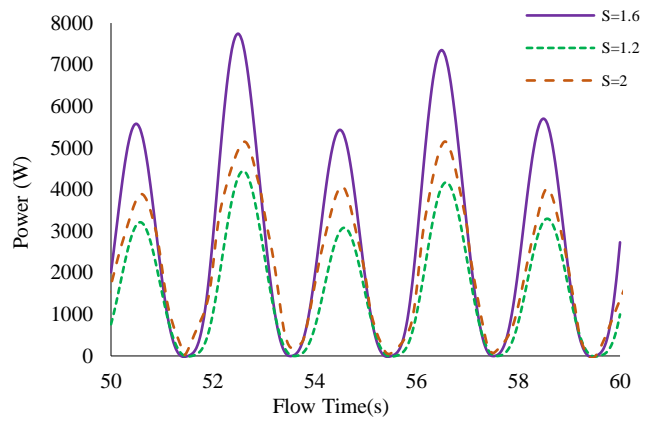
**Fig.14** Time history of pressure for different stroke lengths.

For a given incident wave, the output velocity in vertical direction of the orifice is the greatest when the stroke length is kept at 1.6 m. When stroke length is 1.2, the velocity falls down and when it is further increased to 2 m, the stroke length also falls down as seen in Fig.15.



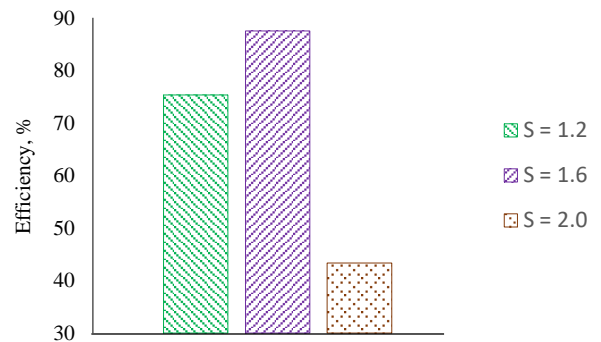
**Fig.15** Time history of velocity for different stroke lengths.

The output power of the wave tank is calculated and presented in Fig.16. It is clearly seen that the output power for  $S = 1.6$  m is maximum while for  $S = 1.2$  and  $S = 2$  is in the second and third place, respectively.



**Fig.16** Time history of power for different stroke lengths.

The efficiency is calculated for different wave properties varying the stroke length of the moving wall. It is seen that maximum efficiency occurs at  $S = 1.6$ , and the value falls down for other two cases ( $S = 1.2$ ,  $S = 2$ ).



**Fig.17** Efficiency of the wave tank for different stroke length.

## 4. Conclusions

The hydrodynamic performance and durability of OWC devices were examined in this thesis using computational fluid dynamics (CFD). The propagating waves were created in a numerical wave tank using a two-phase VOF model and piston type system. The OWC air chamber or column was subsequently fixed at one end. The current numerical model can forecast the motion of the air flow in the duct, variation

of the air pressure in the chamber and oscillation of the free water surface.

- Frontal lip shape has a significant effect on the efficiency of wave tank. So different types of frontal shape are taken into consideration for the analysis. Base shape is the rectangular lip, which is compared with other shapes like rounded lip and triangular lip. It is clearly seen that rounded lip has a greater efficiency than the base shape of the wave tank. But the triangular shape has less efficiency than the base shape of the wave tank.
- The orifice shape is also another factor that has an effect on the pressure developed, velocity, power and the efficiency of the wave tank. Three shapes are considered here: solenoidal, diverging and converging orifice. Solenoidal orifice is taken as the base case. From the plots, it is derived that diverging orifice has less efficiency than the base case and the converging orifice has the higher efficiency than the base case. Diverging orifice has the least efficiency among all the cases.
- Finally, it is also seen that wave height has a significance in the efficiency of the wave tank. There is an optimum value of wave height where the efficiency is maximum for every cases. If the wave height is more or less than the optimum height the efficiency goes down again.

## 5. Acknowledgement

The work is carried out as final year thesis project at KUET and the authors acknowledge the numerical computation facility provided by the Department of Mechanical Engineering, KUET, Bangladesh.

## References

- [1] A. F. de O. Falcão, “Wave energy utilization: A review of the technologies,” *Renewable and Sustainable Energy Reviews*, vol. 14, no. 3, pp. 899–918, 2010.
- [2] S. Zou, O. Abdelkhalik, R. Robinett, G. Bacelli, and D. Wilson. Optimal control of wave energy converters. *Renew Energy*, vol. 103, pp. 217–225, 2017.
- [3] A. Uihlein and D. Magagna, “Wave and tidal current energy – A review of the current state of research beyond technology,” *Renewable and Sustainable Energy Reviews*, vol. 58, pp. 1070–1081, 2016.
- [4] S. Ramezanzadeh, M. Ozbulut, and M. Yildiz, “A Numerical Investigation of the Energy Efficiency Enhancement of Oscillating Water Column Wave Energy Converter Systems,” *Energies (Basel)*, vol. 15, no. 21, p. 8276, 2022.
- [5] Matt Folley, *Numerical Modelling of Wave Energy Converters*. Elsevier, 2016.
- [6] A. Elhanafi, A. Fleming, G. Macfarlane, and Z. Leong, “Numerical hydrodynamic analysis of an offshore stationary–floating oscillating water column–wave energy converter using CFD,” *International Journal of Naval Architecture and Ocean Engineering*, vol. 9, no. 1, pp. 77–99, 2017.
- [7] H. H. Lee, T.-Y. Wu, C.-Y. Lin, and Y.-F. Chiu, “Structural Safety Analysis for an Oscillating Water Column Wave Power Conversion System Installed in Caisson Structure,” *J Mar Sci Eng*, vol. 8, no. 7, p. 506, 2020.
- [8] I. Simonetti, A. Esposito, and L. Cappiotti, “Experimental Proof-of-Concept of a Hybrid Wave Energy Converter Based on Oscillating Water Column and Overtopping Mechanisms,” *Energies (Basel)*, vol. 15, no. 21, p. 8065, 2022.
- [9] H. H. Lee, C.-Y. Wen, and G.-F. Chen, “Study on an Oscillating Water Column Wave Power Converter Installed in an Offshore Jacket Foundation for Wind-Turbine System Part II: Experimental Test on the Converting Efficiency,” *Processes*, vol. 10, no. 2, p. 418, 2022.
- [10] A. Elhanafi and C. J. Kim, “Experimental and numerical investigation on wave height and power take-off damping effects on the hydrodynamic performance of an offshore–stationary OWC wave energy converter,” *Renew Energy*, vol. 125, pp. 518–528, 2018.
- [11] I. Simonetti, L. Cappiotti, H. Elsafti, and H. Oumeraci, “Evaluation of air compressibility effects on the performance of fixed OWC wave energy converters using CFD modelling,” *Renew Energy*, vol. 119, pp. 741–753, 2018.
- [12] C. Xu and Z. Huang, “Three-dimensional CFD simulation of a circular OWC with a nonlinear power-takeoff: Model validation and a discussion on resonant sloshing inside the pneumatic chamber,” *Ocean Engineering*, vol. 176, pp. 184–198, 2019.
- [13] M. Shalby, A. Elhanafi, P. Walker, and D. G. Dorrell, “CFD modelling of a small–scale fixed multi–chamber OWC device,” *Applied Ocean Research*, vol. 88, pp. 37–47, 2019.
- [14] T. Cabral et al., “Performance Assessment of a Hybrid Wave Energy Converter Integrated into a Harbor Breakwater,” *Energies (Basel)*, vol. 13, no. 1, p. 236, 2019.
- [15] C. Wang and Y. Zhang, “Hydrodynamic performance of an offshore Oscillating Water Column device mounted over an immersed horizontal plate: A numerical study,” *Energy*, vol. 222, p. 119964, 2020.
- [16] S. Ringe, “Designing of One Directional Wave Tank,” Uppsala University, 2020.
- [17] D. K. Singh and P. Deb Roy, “Study of water wave in the intermediate depth of water using second-order Stokes wave equation: a numerical simulation approach,” *Sādhanā*, vol. 47, no. 1, p. 45, 2022.
- [18] A. H. Samitha Weerakoon, W. Thilan, H. A. De Silva, and M. Assadi, “Fixed type-oscillating water column front wall angle variation and impact on chamber performance: CFD numerical wave tank assessment,” *IOP Conf Ser Mater Sci Eng*, vol. 1294, no. 1, p. 012015, 2023.
- [19] S. I. Mohsin, and A. Al-Faruk, “Numerical simulation of an oscillating water column device and investigating the effects of lip submergence on velocity and pressure.” *AIP Conf. Proc.*, vol. 2324, no. 1. AIP Publishing, 2021. <https://doi.org/10.1063/5.0037586>
- [20] M. M. Rahman, A. Al-Faruk, M. S. Mahmud, and N. Islam, “Investigating Chamber Geometry and Orifice Diameter of Oscillating Water Column Device by Two Phase CFD Modelling.” *Proceedings of ICME 2023*, Available at SSRN 4889441, 2024.